

Observation of Ultracold-Neutron Production by 9-Å Cold Neutrons in Superfluid Helium

H. Yoshiki,⁽²⁾ K. Sakai,⁽¹⁾ M. Ogura,⁽¹⁾ T. Kawai,⁽³⁾ Y. Masuda,⁽²⁾ T. Nakajima,⁽¹⁾ T. Takayama,⁽¹⁾
S. Tanaka,⁽¹⁾ and A. Yamaguchi⁽¹⁾

⁽¹⁾*Bubble Chamber Physics Laboratory, Tohoku University, Sendai, 980, Japan*

⁽²⁾*National Laboratory for High Energy Physics, Oho, Tsukuba-shi, Ibaraki-ken, 305, Japan*

⁽³⁾*Research Reactor Institute, Kyoto University, Osaka, 590-04, Japan*

(Received 24 October 1991)

Using velocity-analyzed cold neutrons we observed the production of ultracold neutrons in superfluid ^4He at 0.45 to 1.5 K. Ultracold neutrons are produced for an incident neutron wavelength of $8.78 \pm 0.06 \text{ \AA}$ which agrees with the single-phonon emission theory. The temperature variation of the ultracold-neutron storage lifetime is also discussed.

PACS numbers: 61.12.-q, 13.40.Fn, 14.20.Dh, 67.40.-w

It was proposed to produce ultracold neutrons (UCN) by cold-neutron scattering in superfluid ^4He [1] and a number of papers on this process were subsequently published [2-4]. Using panchromatic neutron beams, none of these studies, however, confirmed the characteristic cold-neutron wavelength where this process takes place. According to the single-phonon emission theory [1,5] and using the measured liquid-helium dispersion curve [6,7], this wavelength must be at $8.9 \pm 0.05 \text{ \AA}$, where the error is determined by the variation of the UCN phase-space volume for different wall materials (Fe in this case). The process takes place at a characteristic crossing point of the energy-momentum dispersion curve of superfluid ^4He and the energy-momentum curve of a free neutron (a parabola), where the energy and the momentum of the incoming neutron are converted entirely into those of the phonon produced in superfluid helium.

The UCN are currently believed to be the best tool for searching for an electric dipole moment of the neutron, predicted by the standard model and other theories of particle physics. The strongest present UCN source, operating at Institut Max von Laue-Paul Langevin, consists of a combination of a cold source, a special vertical beamguide, and a turbine [8]. But the idea of using superfluid helium is attractive if cold neutrons can ultimately be allowed to enter the cooling media from all directions.

We have constructed a prototype cryostat [9] called Mark-3000 at KEK for future UCN experiments. Its horizontal UCN container is made of electropolished stainless steel, measuring 3 m in length and 80 mm in diameter. We installed a new ^3He refrigerator [10] in it, capable of cooling 15 liters of purified [10] superfluid ^4He down to 0.45 K. This was first measured in a performance test with heat conduction measurements of the superfluid helium using calibrated Ge thermometers at three separate points in the container [11]. At the lower end of a 6.4-mm-diam polyimide rod, which is inserted in a 40-mm-diam vertical stainless-steel pipe connected to the top of the container and to a turbomolecular high-vacuum pumping system outside, a Yoshiki-type level meter [12], 10 cm long with 1-cm resolution, is mounted.

One of the calibrated Ge thermometers is fixed at the end point of the rod. The rod can be driven up and down vertically via a metal bellows at the top of the pipe. The rod's lowest position serves to measure the liquid level at the time of filling with superfluid liquid He [10], where the Ge thermometer at the end point barely touches the bottom of the container. At an elevated position, 7.5 cm higher, letting the neutron beam pass at the center line of the container for the measurement, it serves to heat up the liquid to a desired temperature by use of a heater built in the level meter. The temperatures thus achieved are extremely stable up to 1.5 K. The final liquid level is adjusted, at the time of filling, in such a way that both the heater and the thermometer at the higher position of the rod are just dipped in the liquid. A number of careful checks were made to ensure that the thermometer readings were exactly the liquid temperatures. This turned out to be indeed so, due to the high heat conductivity of the superfluid [11].

A detector was specially developed for UCN. It is a flat, thin-window ^3He proportional counter with a 40-mm window diameter and 20 mm depth [13]. We developed a technique to mount a 70- μm -thick pure Al window that withstands 6 atm from inside. The ^3He partial pressure is 50 torr, equivalent to 110 and $\frac{1}{4}$ cm in absorption length for thermal and ultracold neutrons, respectively. The rest is filled with pure Ne up to 5 atm to keep the wall effect minimal. Since the expected counting rate is very low, no quenching gas has to be added. The measured efficiency of this counter at 9 \AA is 0.08.

Facing upward, this counter was placed under the electropolished stainless-steel "gravity acceleration" tube extending vertically down from the UCN container. UCN produced in the container gain an energy of about 100 neV by gravity. The end of the acceleration tube is supersealed by a 150- μm -thick Al window, followed by three layers of thermal-shield Al windows. Including the counter window, there are 400 μm of Al between the superfluid helium and ^3He , the counter gas. The attenuation rate, 0.25, was determined by placing dummy Al foils in different thicknesses above the counter. The 30-mm gap above the counter and below the last window is

filled with 1 atm He gas. Two other identical counters, but filled with 1 atm ^3He gas, were placed around the cryostat as background monitors (Fig. 1). At a distance of 52 m from the cold-neutron source of the 20-MW Japan Research Reactor (JRR)-3 at JAERI in Tokai, a pair of beam choppers, 8.13 m apart, was set up. Each chopper consists of a $^6\text{LiF} + \text{B}_4\text{C}$ disk of 38 cm diameter with a 50-mm \times 20-mm slot and a step motor. Both are under the control of a computer program and synchronized at any desired phase-angle difference. They produce a monochromatic beam with 0.82- \AA wavelength width between 3 and 24 \AA . By a slight modification of the program, the front chopper can be a time-controlled beam shutter while the second chopper is kept wide open. The UCN storage lifetime was determined in this way. The cold-neutron intensity at the entrance to Mark-3000 was measured to be 1.1×10^8 neutrons/sec cm 2 .

Figure 2(a) shows what the UCN counter registered at different neutron wavelengths. The ordinate is normalized to the number of incident cold neutrons at the wavelength of the measurement. Since the kinematics and the cross sections for the single-phonon emission process have been analyzed elsewhere (e.g., Refs. [1,5]) we make only a few remarks.

(1) While the entire amount of liquid helium in the container is the source of scattered neutrons, since the upper part of the gravity acceleration tube is surrounded by the ^3He pot and heavy copper walls serving as shields against neutrons [Fig. 1(b)], the UCN counter below, at 90 $^\circ$ to the beam, only "sees" the limited region marked by the ellipse in the container in the figure.

(2) For conduction in the gravity acceleration tube, the critical angle $\theta_c \sim 1.6 \times 10^{-3} \lambda (\text{\AA})$ must be applied to all

neutrons produced around the elliptical region. At 4 \AA incident neutron wavelength, the final-state neutron wavelength is of the same order of magnitude as the incident wavelength and no neutron reflections occur. Thus the counter sees a solid angle given by the cross-sectional area of the gravity tube divided by its length squared, 10^{-3} , and the neutron counting rate is consequently low. As the incident neutron wavelength is increased towards 9 \AA , the number of final-state neutrons reflected from the surface of the tube increases rapidly because the final-state neutron wavelength increases towards infinity (UCN) and the neutron counting rate increases.

(3) Beyond 9 \AA , the final-state neutrons only go forward from kinematics and the counts into the 90 $^\circ$ direction fall off to zero sharply. Therefore the peak shown in Fig. 2(a) does not entirely consist of UCN and is the result of the combined effects of (1) the geometry of the gravity tube and its reflectivity and transmissivity for different wavelengths, (2) the averaging of incident wavelength by the finite resolution of the velocity selector, and (3) the change of counter sensitivity determined by the final-state neutron wavelength. A computer estimate tak-

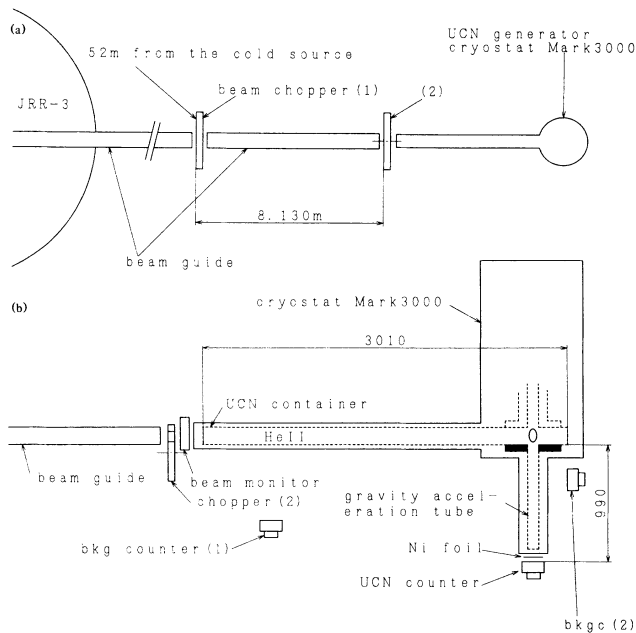


FIG. 1. Experimental layout. (a) Top view and (b) side view.

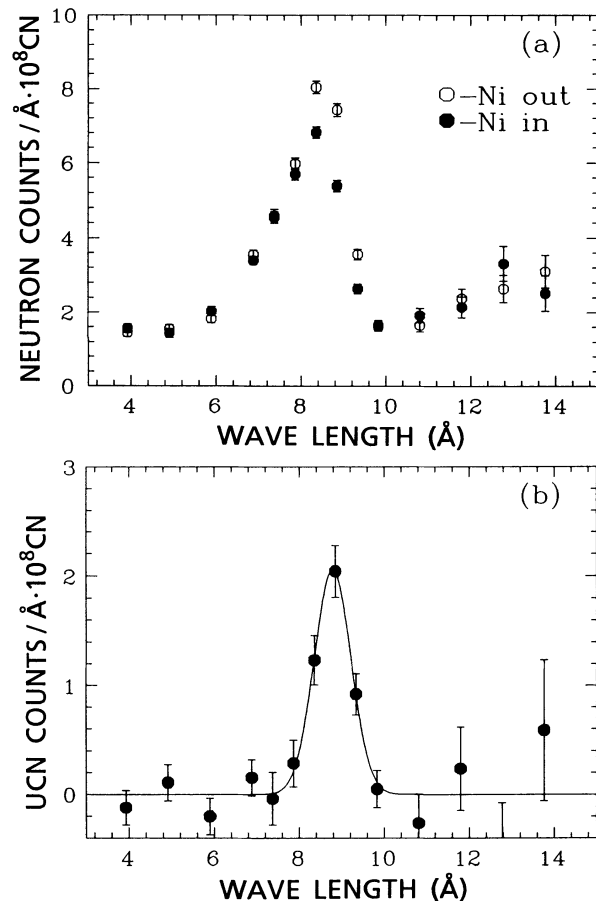


FIG. 2. (a) Counts normalized to incident neutron flux at the wavelength plotted, vs incident wavelength with (solid circles) and without (open circles) Ni foils. (b) UCN yields obtained by subtracting solid from open circles in (a).

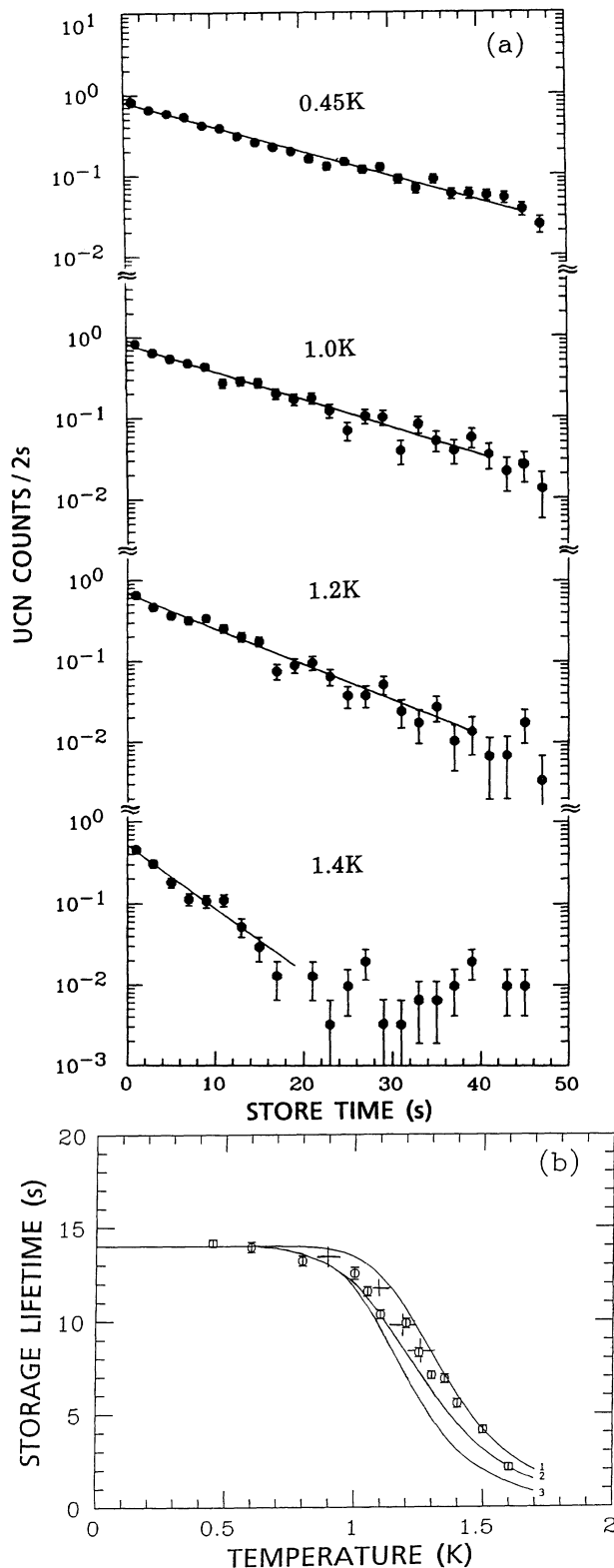


FIG. 3. (a) Distribution of arrival times of UCN at the counter, determining the storage lifetime τ . (b) Temperature dependence of the measured decay time: Four points (+) from Ref. [4] were added after correcting for their different value $\tau_0 = 51$ sec. The solid curves are from Ref. [20] with different A, B, C combinations as in the table.

ing into account these effects has shown a similar curve peaking at 8.5 \AA , but the observed curve is broader than the calculated one, suggesting that the specular reflection assumed in the calculation of the gravity tube is not valid. More elaborate Monte Carlo calculations are in progress. The counts above 10 \AA are almost pure background, increasing as the wavelength increases, because of longer measurement time. In order to filter out UCN we placed $50\text{-}\mu\text{m}$ Ni foils in front of the counter. Ni has a barrier potential of 250 neV and even after gravity acceleration it is shown that 80% of UCN in the container should not pass the foil. The differences in counts with and without Ni foil are shown in Fig. 2(a). We confirmed that the differences are independent of foil thickness ($50, 100,$ and $150 \mu\text{m}$) and are caused by reflection and not by absorption. In Fig. 2(b) the differences are plotted against the incoming neutron wavelength. The UCN production width is 0.1 \AA and the width in the figure is caused by the resolution of the velocity selector, 0.82 \AA . We conclude from a fit that the peak is at $8.78 \pm 0.06 \text{ \AA}$ as predicted by the single-phonon emission theory.

With regard to the variation of UCN storage lifetime with temperature, the measurement cycle consists of 10 sec of an irradiation filling period followed by 50 sec of measurement. We start a multichannel time analyzer at the beginning of a cycle and wait for the chopper to close. The counting rate during this period is flat in time and about 200 times the counting rate right after the chopper is closed. We call the time $t=0$ one second after the chopper is closed. In Fig. 3(a), time distributions of UCN counts after $t=0$ are shown for various temperatures, including exponential decay curves for fitted values of τ . The τ values were replotted in Fig. 3(b) together with four crosses recalculated from Ref. [4]. Since up-scattered neutrons [14] are negligible in our geometry, we conclude that the counts after $t=0$ are UCN except for the background, which amounts to less than 1% below 1 K and 3% at 1.5 K. We used Ni foils as before and measured that only 6% of UCN could pass the foil, in contrast to the 20% expected.

We write

$$\frac{1}{\tau} = \frac{1}{\tau_0} + \frac{1}{\tau(T)},$$

where τ_0 is temperature independent and T is the temperature. τ_0 is 14 sec from Fig. 3(b) and this value is much shorter than expected from surface hydrogen contamination measurements [16–19] since at the very low temperatures, with hydrogen bound tightly to the surface, effective inelastic scattering on hydrogen is small [15]. However, for a UCN gas, one has

$$\tau_{01} = 4V/S\langle v \rangle,$$

where V is the volume of the container, S is the area of a leak, in our case the cross-sectional area of the gravity tube, $\langle v \rangle$ is the average velocity of UCN, and $\tau_0 < \tau_{01}$ must be satisfied. We have $V = 15.1$ liters, $S = 12.5 \text{ cm}^2$,

and $\langle v \rangle = 4.8$ m/sec, yielding $\tau_{01} = 10$ sec, smaller than τ_0 . This contradiction suggests that the gravity tube has a bad conductance, and might give rise to a counterflow of UCN back to the container, among other possibilities. For the temperature-dependent part $1/\tau(T)$ Golub obtained [20]

$$1/\tau(T) = Ae^{-12/T} + BT^7 + CT^{3/2}e^{-8.6/T},$$

where the first term is due to the one-phonon interaction between the UCN and the liquid helium, the second is due to two-phonon processes with one-phonon exchange, and the third is due to roton scattering with one-phonon exchange. Numerically the coefficient of the first term (A) is 500 sec^{-1} if 240 msec^{-1} is used for phonon velocity. A new value of 469 sec^{-1} may be used but it would make no difference in the following discussion. The coefficient of the second term (B) varies slowly with T and Golub gives $(8.8 \text{ and } 7.6) \times 10^{-3} \text{ sec}^{-1}$ at 0.6 and 1.0 K, respectively. 18 sec^{-1} is given for the coefficient of the last term (C). Results of fitting for various combinations of the coefficients are given in the following table:

Curve	A (fixed)	B (fixed)	C (fixed)	Reduced χ^2
1	500	0	0	11.5
2	0	0.008	18	15.8
-	0	0.008	0	7.2
-	0	0	18	25.3
3	500	0.008	18	143.5

We can see the following from the table and Fig. 3(b): (1) It is impossible to fit with the A term only (curve 1). An admixture of the B and possibly C terms is necessary. The best fit is obtained with the B term only. (2) The sum of the three terms A , B , and C makes the calculated storage time too short in comparison with the observed time. Some unknown mechanism similar to $\tau_0 \ll \tau_{01}$ as shown above may be at work. We must ask ourselves about the applicability of Golub's formula to our case because we are measuring the final UCN. But the possibility that the UCN-phonon interaction is weaker than one expects cannot be excluded.

In conclusion, (1) UCN production in superfluid ^4He takes place at the neutron wavelength $8.78 \pm 0.06 \text{ \AA}$ in agreement with the single-phonon emission theory. (2) The T dependence of the storage lifetime can be represented by the equations of Ref. [20], but a more advanced interpretation and a correction of parameters are necessary in order to explain the measured points completely. (3) The poor ratio of the detected UCN to the expected UCN [3,21,22] in this experiment is not well understood. We are left with an unresolved attenuation factor of about 100 in order of magnitude. The main source of attenuation is presumably at the neck of the vertical pipe

and around the four layers of the exit windows [23]. A Monte Carlo calculation is in preparation to clarify this problem. We saw no effect of magnetic field on UCN transmission, at least up to a field of 200 G applied horizontally at the exit.

The authors thank Professor T. Nishikawa, Professor H. Sugawara, Professor H. Hirabayashi, Dr. M. Sakamoto, and all those who gave us indispensable support and invaluable help in performing this project. We also thank Professor V. M. Lobashev and Dr. R. Golub for stimulating discussions. This work has been supported in part by the Inter-University Program for the Common Use of JAERI Facilities.

-
- [1] R. Golub and J. M. Pendlebury, Phys. Lett. **62A**, 337 (1977).
 - [2] P. Ageron, W. Mampe, R. Golub, and J. M. Pendlebury, Phys. Lett. **66A**, 469 (1978).
 - [3] R. Golub, C. Jewell, P. Ageron, W. Mampe, B. Heckel, and A. I. Kilvington, Z. Phys. **B 51**, 187 (1983).
 - [4] A. I. Kilvington, R. Golub, W. Mampe, and P. Ageron, Phys. Lett. A **125**, 416 (1987).
 - [5] M. Cohen and R. P. Feynman, Phys. Rev. **107**, 13 (1957).
 - [6] J. L. Yarnell, G. P. Arnold, P. J. Bendt, and E. C. Kerr, Phys. Rev. **113**, 1379 (1959).
 - [7] D. G. Henshaw, A. D. B. Woods, and B. N. Brockhouse, Bull. Am. Phys. Soc. **5**, 12 (1960).
 - [8] A. Steyerl, H. Nagel, F.-X. Schreiber, K.-A. Steinhäuser, R. Gähler, W. Gläser, P. Ageron, J. M. Asruc, W. Drexel, R. Gervais, and W. Mampe, Phys. Lett. A **116**, 347 (1986).
 - [9] H. Yoshiki *et al.* (to be published).
 - [10] H. Yoshiki (to be published).
 - [11] Y. Fujii *et al.* (to be published).
 - [12] H. Yoshiki, Cryogenics **24**, 704 (1984).
 - [13] H. Yoshiki and H. Yamaguchi (to be published).
 - [14] E. Gutmiedl, R. Golub, and J. Butterworth, Physica (Amsterdam) **169B**, 503 (1991).
 - [15] P. Ageron, W. Mampe, and A. I. Kilvington, Z. Phys. **B 59**, 261 (1985).
 - [16] H. Scheckenhofer and A. Steyerl, Phys. Rev. Lett. **39**, 1310 (1977).
 - [17] W. A. Lanford and R. Golub, Phys. Rev. Lett. **39**, 1509 (1977).
 - [18] J. P. Bugeat and W. Mampe, Z. Phys. **B 35**, 273 (1979).
 - [19] Y. Kawabata, M. Utsuro, S. Hayashi, and H. Yoshiki, Nucl. Instrum. Methods Phys. Res., Sect. B **30**, 557 (1988).
 - [20] R. Golub, Phys. Lett. **72A**, 387 (1979).
 - [21] A. Steyerl and S. S. Malik, Nucl. Instrum. Methods Phys. Res., Sect. A **284**, 200 (1989).
 - [22] P. Ageron and W. Mampe, J. Phys. (Paris), Colloq. **45**, C3-279 (1984).
 - [23] V. M. Lobashev (private communication).